

PHYSICS OF SEMICONDUCTOR DEVICES

Ge/Si Photodiodes with Embedded Arrays of Ge Quantum Dots for the Near Infrared (1.3–1.5 μm) Region

A. I. Yakimov*, A. V. Dvurechenskii, A. I. Nikiforov, S. V. Chaikovskii, and S. A. Tiis

Institute of Semiconductor Physics, Siberian Division, Russian Academy of Sciences, Novosibirsk, 630090 Russia

*e-mail: yakimov@isp.nsc.ru

Submitted January 10, 2003; accepted for publication January 21, 2003

Abstract—A method has been devised for MBE fabrication of $p-i-n$ photodiodes for the spectral range of 1.3–1.5 μm , based on multilayer Ge/Si heterostructures with Ge quantum dots (QDs) on a Si substrate. The sheet density of QDs is $1.2 \times 10^{12} \text{ cm}^{-2}$, and their lateral size is $\sim 8 \text{ nm}$. The lowest room-temperature dark current reported hitherto for Ge/Si photodetectors is achieved ($2 \times 10^{-5} \text{ A/cm}^2$ at 1 V reverse bias). A quantum efficiency of 3% at 1.3 μm wavelength is obtained. © 2003 MAIK “Nauka/Interperiodica”.

1. INTRODUCTION

The efforts in the design of quantum dot (QD) photodetectors began only in the late 1990s, based mainly on InAs/GaAs and Ge/Si heterostructures, and all of them have been concentrated as yet on the production of high-efficiency single elements. QD photodetectors are in a position to cover a significant section of the IR range actual for multiple applications, from the near-IR telecommunication wavelength range (1.3–1.5 μm) to the far-IR spectral range (20–200 μm).

An additional restriction of the carrier motion in the structure plane and discrete energy spectrum of carriers offers a number of significant advantages of QD photodetectors over quantum well (QW) structures and bulk layers [1]:

(i) optical transitions polarized in the photodetector plane become allowed, which opens the possibility for device operation at a normal incidence of light without additional gratings or reflectors;

(ii) oscillator strength (and, consequently, the light absorption coefficient) for intraband and exciton transitions is high owing to localization of the carrier wave function along all three spatial coordinates;

(iii) the lifetime of photoexcited carriers is long ($>10^{-11} \text{ s}$) [2], with the result that the photoelectric gain is high owing to the low capture rate of carriers in a QD. The capture rate is low either because of the absence of allowed energy states between the level in QD and the band of delocalized states or because of the suppression of carrier scattering on optical phonons under the conditions when the energy spacing between the quantum confinement levels exceeds the optical phonon energy.

(iv) dark currents are small (and, consequently, the operating temperature of the photodetector is high). The latter circumstance is a consequence of noninvolvement of excited states in a QD in the processes of thermal generation of carriers in allowed bands in the

case when the energy spacings between the QD levels are sufficiently large.

The most important disadvantages of photodetectors with QD sheets are as follows:

(a) inevitable spread of QD sizes in the array, which results in inhomogeneous broadening of the absorption spectrum and a decrease in the absolute intensity of the photoresponse [2];

(b) low sheet density of QDs (10^9 – 10^{10} cm^{-2}), which is usually by two to three orders of magnitude smaller than the typical electron density in 2D subbands in QW photodetectors (10^{11} – 10^{12} cm^{-2}).

2. FORMULATION OF THE PROBLEM

The elaboration of optical fiber communication lines and related photonic devices operating in the near-IR atmospheric window (1.3–1.5 μm) is one of the most important directions in the development of promising methods for information transmission. It seems necessary to fabricate in one and the same chip the entire set of components of an optical fiber communication line: modulators, demodulators, multiplexers, light emitters, and, naturally, photodetectors. To reduce the cost of such systems it is necessary that all the components be integrated into modern VLSI silicon technology and formed on Si substrates. However, silicon itself is transparent to photons having a wavelength that exceeds 1.1 μm . Germanium photodetectors have a high sensitivity at $\sim 1.5 \mu\text{m}$. This poses the problem of designing Ge/Si heterostructures photosensitive in a range of communication wavelengths of 1.3–1.5 μm at room temperature.

At the first stage, the problem was resolved either by depositing bulk dislocated Ge layers onto Si [3] or by growing multilayer strained superlattices $\text{Ge}_x\text{Si}_{1-x}/\text{Si}$ [4–6]. Standard performance criteria for these photodetectors are the quantum efficiency, and a dark current at

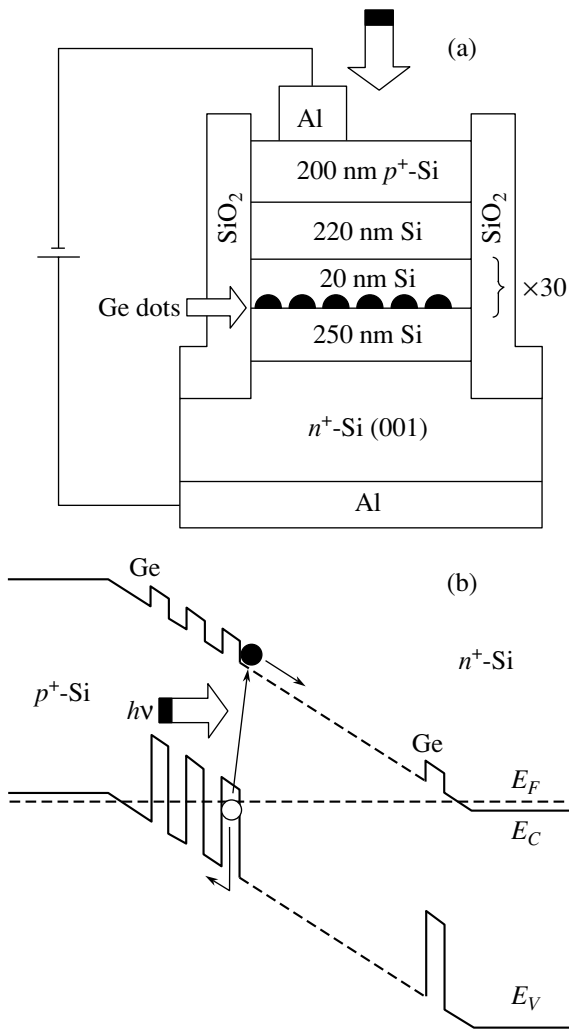


Fig. 1. (a) Sketch of the cross-section of a silicon $p-i-n$ photodiode with Ge QDs; (b) the energy diagram of the diode under zero bias.

a bias of 1 V or the saturation current in diode structures. Similar to the case of long-wavelength photodetectors, a low dark current is necessary to provide low threshold power for the detector.

It was shown that for a photon wavelength of $\lambda = 1.3 \mu\text{m}$, the quantum efficiency of such devices is $\eta = 1-4.2\%$ under normal incidence of light onto the detector, and it can reach $\eta = 11\%$ if the end face of planar waveguides formed on the same Si substrate is illuminated. In the latter case, the transmission of light along GeSi layers and multiple reflection from the waveguide walls made it possible to obtain high η . In spite of the relatively high quantum efficiency, the dark current in bulk and multilayer $\text{Ge}_x\text{Si}_{1-x}/\text{Si}$ heterostructures appeared to be too high. For example, typical dark current densities under a bias of 1 V at room temperature were $10^{-4}-10^{-3} \text{ A/cm}^2$, and the saturation current density was $\sim 10^{-2} \text{ A/cm}^2$, which strongly exceeded currents in Si or Ge $p-n$ diodes.

The next step in the design of high-efficiency Ge/Si photodetectors was the replacement of continuous GeSi layers with sheets of Ge QDs. In view of the prospects for incorporating these elements into Si VLSI circuits, Ge/Si heterostructures with coherently introduced Ge nanoclusters seem the most attractive, since there is the possibility of overgrowing elastically strained Ge layers with structurally perfect Si layers on which other components of a VLSI circuit can be then formed.

The production of waveguide structures based on Si $p-i-n$ diodes with sheets of Ge islands introduced into the diode base was reported in [7, 8]. A quantum efficiency of $\eta = 2.3\%$ was obtained for $\lambda = 1.3 \mu\text{m}$ and a dark current density of $J = 4.2 \times 10^{-4} \text{ A/cm}^2$ under 1-V reverse bias.¹ The authors of [9] reported the production of $p-i-n$ diodes based on Si with Ge nanoclusters, where a maximum quantum efficiency of 8% at a wavelength of $\lambda = 1.46 \mu\text{m}$ and a record-breaking low dark current of $J = 3 \times 10^{-5} \text{ A/cm}^2$ were reached. It is necessary to note that, in the above-cited studies, the density of Ge islands was $\sim 10^9 \text{ cm}^{-2}$ and the islands had a lateral size of about 100 nm and a height of about 10 nm. At so large a size, the splitting of energy levels in the growth plane ($\sim 1 \text{ meV}$), caused by quantum confinement, is much smaller than the room-temperature thermal energy, and, therefore, all the advantages of QD photodetectors over systems of higher dimensionality (e.g., small dark currents) could not be actualized to the fullest extent. It became evident that further improvement of the device parameters demands reduction of the QD size to less than 10 nm with a simultaneous increase in the QD sheet density in order to make the dark current as small as possible without impairing the quantum efficiency of photoconversion.

The goal of the present study was to produce a Ge/Si photodetector containing arrays of Ge QDs with a sheet density at a level of 10^{12} cm^{-2} and a dot size of less than 10 nm, with small dark current and high sensitivity to light at a wavelength of 1.3–1.5 μm .

3. THE TECHNOLOGY OF PHOTODETECTOR FABRICATION

Photodetectors were Si $p-i-n$ diodes, with 30 sheets of Ge QDs, separated by Si spacers 20 nm thick, incorporated into the base (Fig. 1). To reduce the size and increase the density of islands, they were formed on a preliminarily oxidized Si surface.

The samples were MBE-grown on As-doped (001) n^+ -Si substrates with a resistivity of $0.01 \Omega \text{ cm}$. The growth temperature was 500°C for both Si and Ge layers. The growth rate was 0.3 nm s^{-1} for Si and 0.03 nm s^{-1} for Ge. After a standard cleansing of the Si surface, Si buffer layer 250 nm thick was grown. Then oxygen gas was fed into the growth chamber, and Si surface was oxidized for 10 min at an oxygen pressure of 10^{-4} Pa

¹ Here and below the room-temperature parameters of photodetectors are presented.

and a substrate temperature of 500°C. In this process, a SiO_x layer of several angstroms in thickness was formed (not shown in Fig. 1). Further, the chamber was evacuated to a residual oxygen pressure of 10⁻⁷ Pa, a 0.5-nm-thick Ge layer was deposited, and germanium was overgrown with a 20-nm-thick Si layer. The last three procedures (oxidation, deposition of 0.5-nm Ge, deposition of 20-nm Si) were repeated 30 times successively. The multilayer Ge/Si structure was covered with 220-nm Si. The background concentration of B impurity in intentionally undoped Si was (7–8) × 10¹⁵ cm⁻³. The fabrication of *p-i-n* diode was done by growth of 200-nm *p*⁺-Si (B concentration in the layer 2 × 10¹⁸ cm⁻³) and 10-nm *p*⁺⁺-Si (B concentration 10¹⁹ cm⁻³, not shown in Fig. 1).

Aluminum films deposited in a high-vacuum chamber were used to fabricate ohmic contacts to heavily doped Si layers. Columnar diodes were formed by standard photolithography and reactive ion etching of the structures to a depth of ~1.7 μm. The cross-sectional area of mesa-structures varied from 150 × 150 to 700 × 700 μm². The dimensions of Al contact pads on the top *p*⁺-Si layer were 80 × 80 μm². The diode surface was passivated by depositing a 0.5-μm-thick SiO₂ film from an oxygen–monosilane mixture in a special reactor.

The formation of Ge islands and the quality of Si layers were monitored in situ by reflection high-energy electron diffraction (RHEED) (see Fig. 2). After the Si buffer layer growing, the diffraction pattern exhibits reflections from (2 × 1) superstructure typical of atomically clean (001) Si surface. Oxidation changes the diffraction pattern significantly. All the superstructure-related reflections disappear, the bulk reflections become less pronounced, and the diffraction background is more intense. This indicates the formation of a solid SiO_x film on the Si surface. After deposition of Ge onto an oxidized surface, the diffraction pattern typical of 3D Ge islands is observed, with the islands having the same crystallographic orientation as the silicon substrate, indicative of epitaxial growth. Furthermore, it was found that Ge islands are formed in this case after deposition of one Ge monolayer (ML) without the formation of the underlayer typical of the Stranski–Krastanow growth mechanism. Therefore, Ge nanoclusters in this system are completely isolated from one the other. This fact seems especially important, since the presence of 2D states in the underlayer can significantly accelerate capture of carriers in QDs [10, 11].

The mechanism of the formation of Ge islands in Ge/SiO_x/Si system has yet to be explained. The most probable hypothesis is that, at the early stage of growth, GeO and SiO molecules are formed in the reaction of Ge adatoms with a SiO₂ film; leaving the surface, these molecules uncover Si areas on which Ge nanoclusters are then nucleated [12].

Figure 3a shows an SEM image of a (001) Ge/Si surface formed after deposition of a single Ge layer of

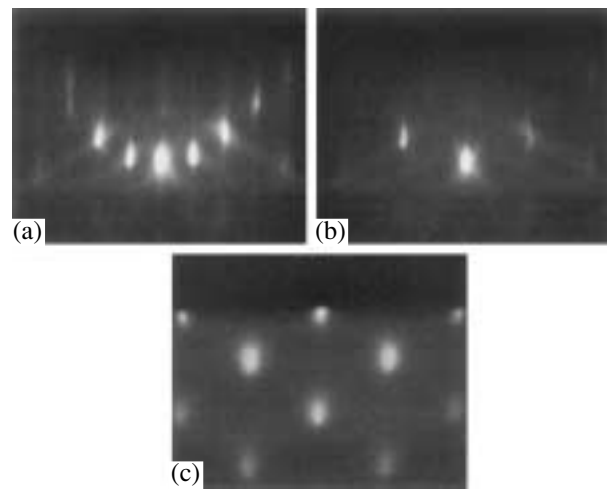


Fig. 2. RHEED pattern from the sample surface at different growth stages: (a) (001) Si (2 × 1) after growth of an Si buffer layer; (b) (001) Si (1 × 1) after oxidation in O₂ flow; (c) 3D diffraction after deposition of 0.5-nm Ge.

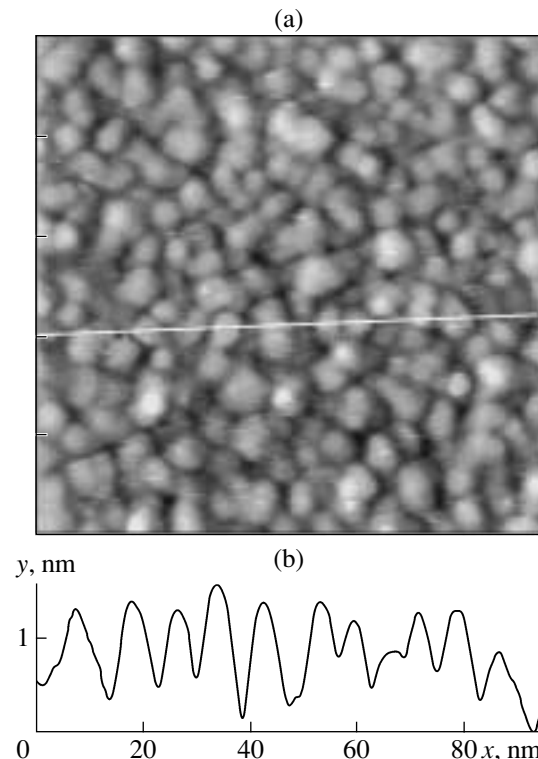


Fig. 3. (a) SEM image of the Si surface after deposition of a 0.5-nm Ge layer. An image size of 100 × 100 nm²; (b) The surface profile along the line is marked in Fig. 3a.

0.5 nm in thickness. As seen, the surface represents an array of islands, and Figure 3b shows their profile in the direction marked by the line in Fig. 3a. Statistical processing of the surface profiles yielded an average lateral size of Ge islands of ~8 nm and a density of ~1.2 × 10¹² cm⁻².

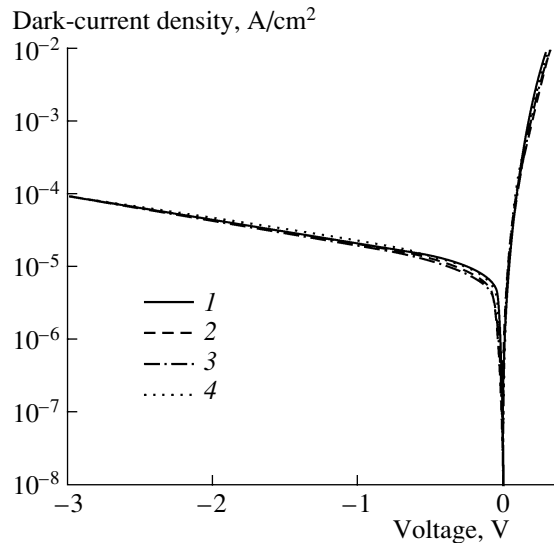


Fig. 4. Dark J - V characteristics of photodiodes with cross-sectional areas of (1) 700×700 , (2) 500×500 , (3) 300×300 , and (4) $150 \times 150 \mu\text{m}^2$. Recorded at $T = 300 \text{ K}$.

4. DARK-CURRENT-VOLTAGE CHARACTERISTICS

Figure 4 shows the dark current density vs. voltage (J - V characteristics) at room temperature for diodes differing in area. The current density is virtually independent of the diode area, which is indicative of small surface leakage and predominance of bulk processes in the charge transport. An ideality factor of $n = 1.02$ and a saturation current density of $J_s = 6 \times 10^{-6} \text{ A/cm}^2$ were determined from J - V characteristics. The ideality factor is close to unity, which indicates the absence of any considerable contribution of tunneling and recombination currents related to possible deep centers in the diode base. The saturation current density is one to two orders of magnitude smaller than that in p - and p - i - n diodes (10^{-4} - 10^{-3} A/cm^2) [13], which implies that the energy gap in a QD Ge/Si heterostructure is wider than in bulk Ge, to all appearances due to confinement-induced quantization of the energy spectrum of holes in the Ge valence band.

The dark current density at 1-V reverse bias was $2 \times 10^{-5} \text{ A/cm}^2$. To our knowledge, this is the lowest value achieved hitherto for Ge/Si photodetectors.

5. PHOTOELECTRIC PROPERTIES

Figure 5 shows typical current responsivity spectra at different reverse biases under normal incidence of light onto the photodetector surface. The measurements were made at room temperature. The photocurrent in the short-circuit mode (a bias of $U = 0$) was measured directly with a Keithley electrometer. The photoresponse of reverse-biased photodiodes was measured using a lock-in nanovoltmeter at a light-modulation frequency of 560 Hz. The spectral characteristics of illu-

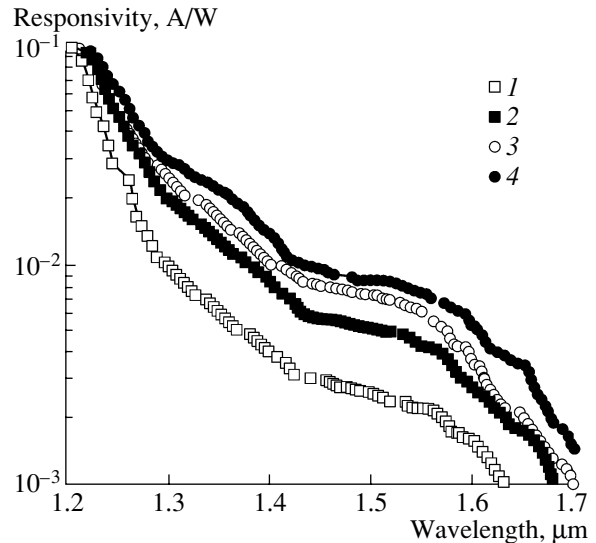


Fig. 5. Current responsivity spectra at varied reverse bias on the photodiode $|U|$: (1) 0 (short-circuit mode), (2) 0.2, (3) 0.5, and (4) 2 V. Recorded at room temperature.

mination intensity were obtained using a cooled CdHgTe photoresistor. As seen, the photosensitivity of a QD Ge/Si p - i - n diode in near-IR range extends to wavelengths of 1.6–1.7 μm .

Figure 6 shows the dependence of quantum efficiency η at a wavelength of $\lambda = 1.3 \mu\text{m}$ on the reverse bias. The value of η was calculated from the known relation between the sensitivity R , photon energy $h\nu$, and elementary charge: $R = (e/h\nu)\eta$. With increasing bias, the quantum efficiency increases and levels off at $|U| \approx 2 \text{ V}$. Study of capacitance-voltage (C - V) characteristics of diodes has shown that the device capaci-

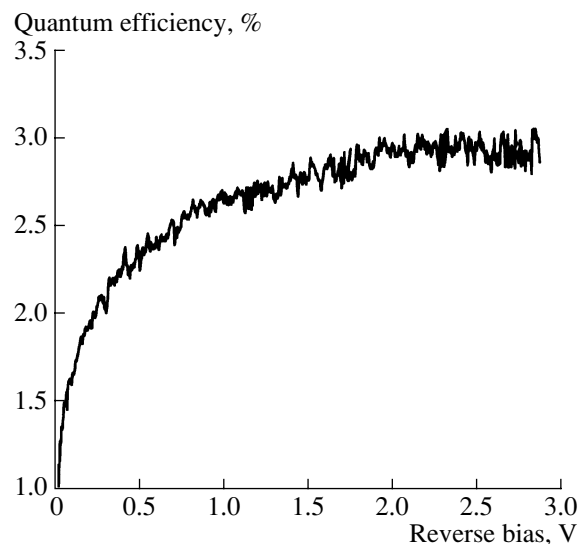


Fig. 6. The quantum efficiency of a photodiode at a wavelength of 1.3 μm vs. reverse bias.

tance remains unchanged within a 5% accuracy in the reverse bias range $|0-5|$ V. This means that the entire i -layer lies within the space-charge region of ionized residual boron impurities and QDs do not contain holes (otherwise, the recharging of QDs with increasing $|U|$ would give rise to features in the $C-V$ characteristics [14]). Consequently, all 30 sheets of Ge QDs can be involved in the band-to-band absorption of light even in the unbiased state, and it might seem that further rise of the reverse bias must not lead to any increase in η .

The increase in the quantum efficiency in electric field can be explained as follows. It is known that the Ge/Si heterojunction is of type II, since the lowest energy state for electrons lies in the Si conduction band, and the lowest state for holes, in the Ge conduction band (Fig. 1b) [14]. The absorption of photons with energy lower than the energy gap of Si gives rise to electron transitions from the Ge valence band to the Si conduction band. In this process, free electrons appear in the Si conduction band, and holes, in Ge islands. Since holes are localized in Ge QDs, electrons make the major contribution to photocurrent at low electric field. At high voltage, holes can effectively tunnel from localized states in QDs to the Si valence band; thus, the photocurrent increases. Evidently, in a sufficiently strong electric field, when all the photoholes can move away from QDs, the photoresponse levels off.

Maximum quantum efficiency of detectors was 3%, which is close to the values obtained for photodetectors based on strained multilayer $\text{Ge}_x\text{Si}_{1-x}/\text{Si}$ superlattices. Further increase in quantum efficiency can be reached by designing a detector with a waveguide structure which uses the effect of multiple internal reflection, e.g., on a silicon-on-insulator substrate.

6. CONCLUSIONS

The main results of this study are as follows.

(1) A method has been devised for fabrication of silicon $p-i-n$ photodiodes for the near-IR (1.3–1.5 μm) range with incorporated sheets of Ge QDs; with a sheet density of QDs higher than 10^{12} cm^{-2} , the dot size less than 10 nm.

(2) The lowest reported dark current density, $2 \times 10^{-5} \text{ A/cm}^2$ under reverse bias of 1 V at room temperature, has been achieved in these detectors.

(3) Quantum efficiency under normal incidence of light onto photodiode reaches 3%, which is close to the values obtained for photodetectors based on strained multilayer $\text{Ge}_x\text{Si}_{1-x}/\text{Si}$ superlattices.

ACKNOWLEDGMENTS

We are grateful to N.P. Stepina for her assistance in the preparation of samples, and to A.E. Klimov and I.B. Chistokhin for technical assistance.

The study was supported by the program of the Ministry of Industry, Science, and Technology of the Russian Federation (project no. 01.200.113897), INTAS (project no. 2001-0615), and the Russian Foundation for Basic Research (project no. 03-02-16526).

REFERENCES

1. V. Ryzhii, *Semicond. Sci. Technol.* **11**, 759 (1996).
2. J. Phillips, *J. Appl. Phys.* **91**, 4590 (2002).
3. L. Colace, G. Masini, G. Assanto, *et al.*, *Appl. Phys. Lett.* **76**, 1231 (2000).
4. F. Y. Huang, X. Zhu, M. O. Tanner, and K. Wang, *Appl. Phys. Lett.* **67**, 566 (1995).
5. H. Presting, *Thin Solid Films* **321**, 186 (1998).
6. C. Li, C. J. Huang, B. Cheng, *et al.*, *J. Appl. Phys.* **92**, 1718 (2002).
7. M. Elcurdi, P. Boucaud, S. Sauvage, *et al.*, *Appl. Phys. Lett.* **80**, 509 (2002).
8. M. Elcurdi, P. Boucaud, S. Sauvage, *et al.*, *J. Appl. Phys.* **92**, 1858 (2002).
9. S. Tong, J. L. Wan, and K. Wang, *Appl. Phys. Lett.* **80**, 1189 (2002).
10. D. Morris, N. Perret, and S. Fafard, *Appl. Phys. Lett.* **75**, 3593 (1999).
11. Y. Yoda, O. Moriwaki, M. Nishioka, and Y. Arakawa, *Phys. Rev. Lett.* **82**, 4114 (1999).
12. A. A. Shklyayev, M. Shibata, and M. Ichikawa, *Phys. Rev. B* **62**, 1540 (2000).
13. G. E. Pikus, *Fundamentals of the Theory of Semiconductor Devices* (Nauka, Moscow, 1965), p. 207.
14. A. I. Yakimov, N. P. Stepina, A. V. Dvurechenskii, *et al.*, *Semicond. Sci. Technol.* **15**, 1125 (2000).

Translated by D. Mashovets